CrystEngComm

Accepted Manuscript

ROYAL SOCIETY OF CHEMISTRY

www.rsc.org/crystengcomm

Journal Name

RSCPublishing

ARTICLE

Enhanced gas-sorption properties of a high surface area, ultramicroporous magnesium formate

Cite this: DOI: 10.1039/xoxxoooooox

Received ooth January 2012,
Accepted ooth January 2012

DOI: 10.1039/xoxxoooooox

www.rsc.org/

I. Spanopoulos,[a] I. Bratsos,[b] Ch. Tampaxis,[b] A. Kourtellaris,[c] G. Charalambopoulou,[b] T.A. Steriotis[b] and P.N. Trikalitis*[a]

The direct solvothermal reaction of $Mg(NO_3)_2.6H2O$ in dimethylformamide at 130 °C leads to the formation of highly crystalline α-$[Mg_3(O_2CH)_6]$ with an expanded unit cell. Successful pore activation was performed after heating the material at 240 °C under dynamic vacuum. In contrast to literature reports, the pores in the activated solid are accessible to nitrogen molecules and the corresponding BET surface area is 496 $m^2 g^{-1}$, very close to the geometric area calculated from the single crystal structure. A detailed gas-sorption study (N_2, Ar, H_2, CO_2, CH_4 and NH_3) is reported. The material is ammonia stable showing a reversible uptake of 5.4 mmol g^{-1} at 298 K, while the corresponding CO_2 uptake is 2.2 mmol g^{-1} with moderate CO_2/CH_4 (4.6) selectivity but high CO_2/N_2 (23) and CH_4/N_2 (5.2) selectivity. The latter is among the highest values reported up to date in the entire family of porous materials. The H_2 uptake at 77 K is 1.2 wt% which is the highest among the reported values for various magnesium formates.

INTRODUCTION

Metal-organic frameworks (MOFs) are crystalline nanoporous materials comprised of metal ions or clusters connected three-dimensionally by multi-topic organic ligands. This hybrid architecture opens the possibility to design and synthesize a great variety of new porous materials.[1,2] However, many MOFs are sensitive to moisture, limiting in this way their potential utilization in industrial applications. To overcome this problem the use of small, hard metal ions (Mg^{2+}, Al^{3+}) in MOF synthesis can be utilized leading to air and water stable materials.[3,4] Additionally the use of light metal ions in MOF synthesis can result in lightweight materials, a prerequisite for the application of porous compounds in real gas storage applications.[5,6] Compared to the vast number of MOFs, magnesium-based porous analogues are rare. The high affinity of Mg^{2+} towards the oxygen donor atoms from H_2O and other polar solvents including dimethylformamide (DMF), prohibits the formation of open framework solids, under hydro(solvo)thermal reaction conditions using carboxylate-based organic linkers. A representative example is Mg-MOF-74, an air stable MOF, with a remarkable CO_2 uptake of 35.2 wt % at 1 bar and 296 K and also high H_2 uptake reaching 1.96 wt % at 1 bar and 77 K.[7]

Another important Mg-based MOF is the microporous magnesium formate, $Mg_3(O_2CH)_6$. Three polymorphs α-,[8] β-[9] and γ-$Mg_3(O_2CH)_6$[10] have been reported, from which the α-polymorph has attracted more attention because it is easy to prepare. This MOF is also commercially available.[11] However, in terms of its gas-sorption properties there are contradictory and confusing results. For example, a very low accessible surface area (measured by N_2 adsorption at 77 K) is reported by Banerjee et al.[10], Henderson et al.[8] as well as by Hirscher et al.,[12] while Kim et. al,[13] reported a significant N_2 adsorption at 77 K (116 $cm^3 g^{-1}$) but no other gas-sorption properties for this material. In fact, α-$Mg_3(O_2CH)_6$ is considered as a molecular sieve because it was reported that can discriminate N_2 by H_2 due to its very small pore size.[12] At the same time, it has been demonstrated that a great variety of solvent molecules, including DMF, benzene, THF, MeOH, EtOH, Me_2CO and Et_2O can readily occupy the pore space.[8] The different size of the solvent molecule results in a different unit cell volume in the range 1611.6(18) $Å^3$ - 1707.2(3) $Å^3$, demonstrating the flexibility of the framework. Taking into account the relative sizes of these solvent molecules it would be expected that the pore space of α-$Mg_3(O_2CH)_6$ will be readily accessible for small gas molecules like N_2 and therefore limited size selectivity is anticipated. It is therefore evident that the reported gas-sorption properties of α-$Mg_3(O_2CH)_6$ are not representative of the guest-free material and as we explain below this is attributed mainly to an unsuccessful activation procedure.

We report here that α-$Mg_3(O_2CH)_6$ with an expanded unit cell (1704.4 $Å^3$) can be readily synthesized by heating $Mg(NO_3)_2{\cdot}6H_2O$ in DMF at 130 °C. Notably, this is an almost

4% increase of the unit cell volume compared to the previously reported value for α-$Mg_3(O_2CH)_6$ (1640.9 $Å^3$)[8] synthesized in DMF but at lower temperatures (110 ^oC), demonstrating the flexibility of the framework. Single crystal and powder X-ray diffraction experiments, in both the as-made and the evacuated solid, revealed the structure and confirmed the purity of the material. As we demonstrate below, heating of the material at 240 ^oC under dynamic vacuum is crucial to obtain a fully activated solid. ^1H NMR spectroscopy validated the complete removal of residual solvents for the evacuated material. Evaluation of the thermal stability of the material was confirmed by TGA analyses. More important, the structure of the evacuated solid was determined by single-crystal X-ray diffraction and found to be slightly contracted having a unit cell volume of 1641.7 $Å^3$. Remarkably, the structure expands back to the original size upon DMF insertion. Extensive and detailed gas-sorption (N_2, Ar, H_2, CO_2, CH_4, and NH_3) studies were performed. The experimentally determined BET area is 486 m^2 g^{-1} (Langmuir 509 m^2 g^{-1}, Ar at 87 K) which is very close to the geometric surface area (432 m^2 g^{-1}) calculated from the single crystal structure (Ar probe molecule) of the evacuated solid.[14] As we present below the gas adsorption properties of the present, high surface area α-$Mg_3(O_2CH)_6$ are improved compared to previous reports. For example, the saturation H_2 uptake at 77 K and 27 bar is 1.2 wt% which is 10% higher than the previously reported value (1.1 wt% at 77 K and 20 bar). In addition we report for the first time in the microporous magnesium formate family, on CO_2/CH_4, CO_2/N_2 and CH_4/N_2 selectivity as well as on NH_3 adsorption.

EXPERIMENTAL SECTION

Starting Materials. All chemicals were purchased and used without further purification. $Mg(NO_3)_2{\cdot}6H_2O$ was purchased from Alfa Aesar and dimethyformamide (DMF) was purchased from Scharlau.

Synthesis of α-[$Mg_3(O_2CH)_6$] (**1**). A solution of 5 mL DMF and 0.070 g of $Mg(NO_3)_2{\cdot}6H_2O$ was placed in a 20 mL glass scintillation vial. The vial was sealed and placed in an isothermal oven at 130 °C for 5 days. During this period, high quality colorless cubic crystals of **1** were deposited (50% yield based on $Mg(NO_3)_2{\cdot}6H_2O$).

Structural characterization. As-made material (1): Single-crystal X-ray diffraction (SXRD) data were collected at 250 K on a STOE IPDS II diffractometer operated at 2000 W power (50 kV, 40 mA) with graphite monochromatized MoKα (λ= 0.71073 Å) radiation. An analytical absorption correction was applied using the program X-RED (routine within the X-AREA software package). Data reduction was performed with the APEX2 software, SAINT and SADABS. All structures were solved by direct methods and refined with SHELXL software.[15] All other non-hydrogen atoms were refined anisotropically. Hydrogen atoms were generated with idealized geometries. The solvent, DMF guest molecules were located and resolved in the pores. CCDC 1019005.

Activated, solvent free material (1'): SXRD data of the activated solid (the activation procedure is described below in the Gas-sorption measurement section) were collected at 250 K on an Oxford-Diffraction Supernova diffractometer, equipped with a CCD area detector utilizing Cu Kα (λ = (1.5418 Å) radiation. Suitable crystals were attached to glass fibers using paratone-N oil and transferred to a goniostat where they were cooled for data collection. Empirical absorption corrections (multiscan based on symmetry-related measurements) were applied using CrysAlis RED software.[16] The structures were solved by direct methods using SIR2004[17] and refined on F^2 using full-matrix least-squares with SHELXL97. CrysAlis RED for cell refinement and data reduction and WINGX for geometric calculations.[18] CCDC 1031592.

Powder X-ray diffraction patterns (PXRD) were collected on a Panalytical X'pert Pro MPD system (CuKα radiation) operated at 45 kV and 40 mA. A typical scan rate was 5 sec/step with a step size of 0.01 deg. Simulated PXRD patterns were calculated from the corresponding single crystal data using the program Mercury from CCDC[19]. Thermogravimetric analyses (TGA) were performed using a TA SDT Q 600 analysis system. An amount of 20 mg of sample was placed inside an alumina cup and heated up to 650 ^oC under Argon flow with a heating rate of 5 ^oC/min. ^1H NMR spectra were recorded on a Bruker 300 MHz spectrometer, in D_2O solutions.

Gas sorption measurements

Low-pressure nitrogen, argon, hydrogen, carbon dioxide, methane and ammonia sorption measurements were carried out on an Autosorb 1-MP instrument from Quantachrome equipped with multiple pressure transducers for highly accurate analyses and an oil-free vacuum system. High pressure excess adsorption measurements were conducted manometrically on a PCTPro-2000 instrument (Setaram) with the aid of a regular valve sealed stainless-steel measuring cell. The NIST database was implemented for estimating the compressibility of gases (H_2, CH_4, CO_2) and helium was used for dead volume calibrations at 273-303K. In order to avoid helium sorption errors, the dead volume at 77K was calculated through a reference curve obtained by using different volumes of non adsorbing material (pyrex glass).

Ultra-high purity grade N_2 (99.999%), Ar (99.999%), He (99.999%), H_2 (99.999%), CO_2 (99.999%), CH_4 (99.9995%) and NH_3 (99.999%), were used for all adsorption measurements. Prior to analysis, as-made samples were soaked in absolute ethanol at room temperature for three (3) days during of which the supernatant solution was replaced six (6) times. The ethanol suspended samples were transferred inside the chamber of a supercritical CO_2 dryer (Bal-Tec CPD 030) and ethanol was exchanged with liquid CO_2 over a period of 5 hours at 8 ^oC. During this period, liquid CO_2 was vented under positive pressure every 5 minutes. The rate of CO_2 venting was always kept below the rate of filling so as to maintain full drying conditions inside the chamber. Following venting, the temperature was raised to 40 ºC (above the critical temperature of CO_2), kept there for 1 hour and then slowly vented over the period of 1 hour. The dried sample was transferred immediately inside a pre-weighted, Argon filled 9 mm cell and closed using

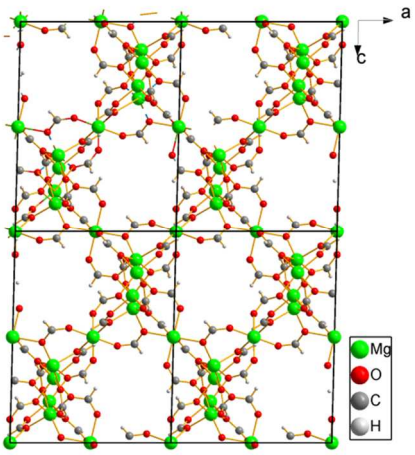

Fig. 1 The structure of **1** looking down the *b*-axis.

CellSeal™ provided by Quantachrome to prevent intrusion of oxygen and atmospheric moisture during transfers and weighing. The cell was then transferred to the outgassing station where the sample was evacuated under dynamic vacuum at room temperature until the outgas rate was less than 2 mTorr/min. After evacuation, the sample and cell were re-weighed to obtain the precise mass of the evacuated sample. Finally, the tube was transferred to the analysis port of the gas adsorption instrument.

RESULTS AND DISCUSSION

Synthesis and structure determination

In the magnesium formate system, three polymorphs *α*-, *β*- and *γ*- have been reported each one synthesized by a different synthetic routes.[8,9,10] In contrast to the previously reported methods, the synthesis of the present *α*-$[Mg_3(O_2CH)_6]$ was performed in DMF without the use of formic acid. The later was generated in-situ from the decomposition of DMF[20] at the elevated reaction temperature (130 °C). Large cubic crystals were formed, suitable for single crystal X-ray diffraction measurements. Phase purity was confirmed by powder X-ray diffraction (see Fig. S1). Compound **1** crystallizes in the monoclinic system (space group $P2_1/n$) with unit cell parameters a = 11.416(2) Å, b = 10.013(2) Å, c = 14.914(3) Å, β = 91.44(3)° (V = 1704.4(6) Å^3) and chemical formula $[Mg_3(O_2CH)_6](DMF)$. This is isostructural to the previously reported *α*-$[Mg_3(O_2CH)_6](DMF)$[8] and contains edge-sharedMgO$_6$ octahedra that are linked together by corner-sharing octahedra, leading to a three dimensional structure. This connectivity results in the formation of one dimensional channels running along the *b*-axis, in which DMF molecules reside, see Fig. 1. However, the unit cell is found significantly expanded compared to the reported *α*-$[Mg_3(O_2CH)_6](DMF)$.[8a] More specifically, the large difference was found in the *c*-axis length which is elongated by 0.378 Å (the *a* and *b*-axis are elongated by 0.015 Å and 0.108 Å respectively), leading to an increase in the unit cell volume by 4 %. This enlargement is also reflected in the void space of **1.** Accordingly, using PLATON[21] the accessible volume in **1** after excluding the DMF molecules, is 34% which is 10% higher compared to the reported value (30.9 %).[8] Looking at the Mg-O bond lengths, these were found on average longer in **1**, 2.086 Å versus 2.075 Å.

The observed unit cell expansion demonstrates the flexibility of the framework in **1**, presumably caused by the higher reaction temperature (130 °C versus 110 °C). This is very interesting because usually higher reaction temperatures result in more dense phases. Therefore **1** may be considered as a new, kinetically stabilized phase of *α*-$[Mg_3(O_2CH)_6](DMF)$ with an increased void volume. As we present below, this void volume is readily accessible by small gas molecules, after DMF is removed from the channels.

The structure of the solvent-free material, **1'**, is determined by SXRD. Accordingly, **1'** is isostructural to **1** containing no solvent molecules with an intact framework, however the unit cell volume is contracted by 3.65% (from 1704.4(6) Å^3 to 1641.67(14) Å^3).[22] This is also confirmed by powder XRD, see Fig. S1c,d. Remarkably, upon insertion of DMF, **1'** expands back to **1** indicating a breathing behavior of the framework, see Fig. S1e. The refined unit cell of the re-solvated material is a = 11.393(2) Å, b = 10.034(4) Å, c = 14.915(4) Å, β=91.440°, V = 1704.5 Å^3. These values are very close with that of the as-made solid, **1**. Using PLATON, the accessible volume in **1'** is 32%.

Gas-sorption properties

The guest DMF molecules in **1** were successfully removed without structural damage by supercritical CO_2 activation (sc-CO_2). This is the most "soft" activation procedure that can produce high surface area MOFs minimizing structural deformation or damage, even in the case of very fragile frameworks.[23,24] Before sc-CO_2 activation, DMF was exchanged with EtOH. At this stage, complete DMF removal was confirmed by ^{1}H NMR in an acid digested sample, see Fig. S2. An important finding is that after CO_2 activation, the high surface area materials can only be obtained after thermal heating at 240 °C under high vacuum. Lower degassing temperatures resulted in significantly reduced surface area. Initially, it was expected that after CO_2 activation the solid would be dry, free of EtOH and therefore no heating under

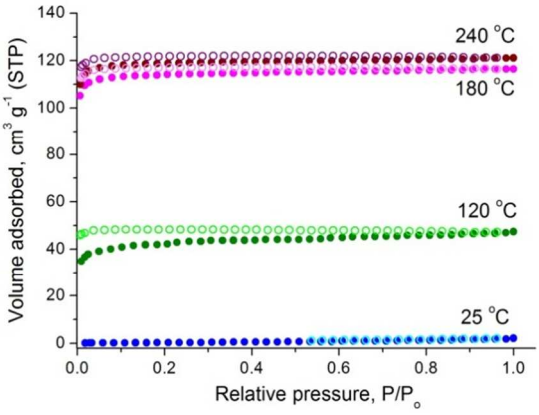

Fig. 2 Nitrogen adsorption (closed symbols) and desorption (open symbols) isotherms of **1'** at different activation temperatures, recorded at 77 K.

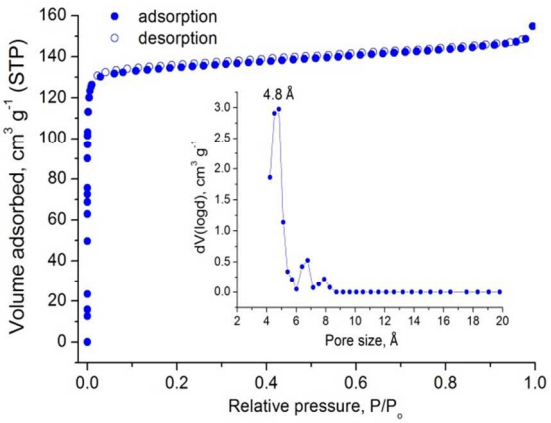

Fig. 3 Detailed, microporous Ar sorption isotherms of **1'** recorded at 87 K. Inset shows the corresponding NLDFT pore distribution curve.

vacuum was scheduled. Accordingly, the material was kept under vacuum overnight at room temperature and then transferred to the analysis station. As shown in Fig. 2, no N_2 adsorption at 77 K was observed suggesting no pore accessibility. We then heated the material progressively at 120 ^oC, 180 ^oC and 240 ^oC. After each thermal treatment, N_2 sorption isotherms were recorded at 77 K, see Fig. 2. The maximum N_2 uptake, corresponding to the maximum surface area and pore volume was observed at 240 ^oC. We avoided heating the material at higher temperatures to prevent possible structural deformation and because the BET surface area was found to be 496 $m^2\ g^{-1}$ (total pore volume, 0.19 $cm^3\ g^{-1}$), which is even higher than the geometric surface area calculated from the single crystal structure of **1'** (432 $m^2\ g^{-1}$).[14,25] We note however that based on thermogravimetric analysis (TGA) data, the framework is stable up to 400 ^oC (see Fig. S4). In a controlled experiment, we heated an EtOH exchanged material to 240 ^oC overnight (heating rate 1 deg min^{-1}) and we found a lower N_2 uptake (97.1 $cm^3\ g^{-1}$ at 0.3 P/P_o vs. 119.5 $cm^3\ g^{-1}$ at the same relative pressure for the sc-CO_2 activated **1'**, see Fig. S9), suggesting that sc-CO_2 activation has a positive effect in activating **1**, in agreement with literature reports.[23,24]

Detailed microporous analysis using Ar adsorption at 87 K revealed an almost identical BET area (486 $m^2\ g^{-1}$) with a total pore volume of 0.19 $cm^3\ g^{-1}$ and a narrow pore size distribution centered at 4.8 Å, see Fig. 3. The increased pore size in **1'** may explain to an extent the accessibility by N_2 and Ar gas molecules, in contrast to the non-accessible by these gasses α-$[Mg_3(O_2CH)_6]$ with a 3.7 Å pore size.[8,12] However, looking at the N_2 adsorption isotherm, an evident low pressure hysteresis is observed in all cases, although this is reduced for the material activated at 240 ^oC. This kind of hysteresis is usually associated with reduced diffusion kinetics of the gas molecules due to the very small pore size. Indeed, the kinetic data presented in Fig. S10 for representative relative pressure points, clearly show that there is no equilibrium but a gradual decrease of the pressure of the gas above the sample, even after 14 minutes (the equilibrium time was set at 3 minutes). It is well documented[26] that for ultramicroporous solids (pore widths < 7 Å) the rate of N_2 adsorption and equilibration is very slow (a bilayer of N_2 molecules is ~ 7 Å) and therefore under-equilibration is likely to occur. The use of Ar at 87 K significantly reduces this problem (see Fig. 3) because of its smaller kinetic diameter (3.4 Å) and also the reduced attractive interactions with the pore walls as compared to N_2.[27]

For comparison purposes we also measured the commercially available[11] α-$[Mg_3(O_2CH)_6]$ following our optimized degassing procedure (240 ^oC for overnight). Surprisingly and in contrast to a previous report[12], a high nitrogen uptake is observed at 77 K (107 $cm^3\ g^{-1}$ at 0.95 P/Po) as shown in Fig. S9. In particular, the BET surface area was found to be 336 $m^2\ g^{-1}$ (Langmuir 442 $m^2\ g^{-1}$), significantly higher compared to the reported values (BET 16 $m^2\ g^{-1}$ and Langmuir 24 $m^2\ g^{-1}$). However, these values are lower compared to **1'** because the former has a reduced unit cell volume (1617 $Å^3$ versus 1641.7 $Å^3$ in **1'**).[27] Therefore, our results strongly suggest that the thermal activation procedure in α-$[Mg_3(O_2CH)_6]$ is essential for obtaining a high surface area solid. Also important, the magnitude of this surface area is a function of the unit cell volume of the material.

The high porosity of **1'** prompted us to investigate important gas sorption properties by recording low and high pressure isotherms of H_2, CO_2, CH_4 and NH_3 at different temperatures from which isosteric heat of adsorption (Q_{st}) and CO_2/CH_4, CO_2/N_2 and CH_4/N_2 selectivity is calculated. It is important to mention that before each measurement the material had to be reactivated at 240 ^oC otherwise the adsorption capacity was significantly lower. More specifically, after the initial activation at 240 ^oC and the verification for accessible porosity (N_2 at 77 K, see Fig. 2), we first recorded a hydrogen sorption isotherm at 77 K. A fully reversible isotherm was obtained as shown in Fig. S5. Immediately after, we executed a micropore analysis for accurate determination of pore size distribution, using Ar at 87 K. Surprisingly, a low Ar adsorption was measured, suggesting limited accessibility in the pore space, see Fig. S6. By heating this material at 240 ^oC under vacuum for 12 h, the expected accessible porosity with a type-I isotherm (BET area, 486 $m^2\ g^{-1}$), typical for microporous materials, was found (see Fig. 3). We then run a H_2 sorption at 87 K, in order to calculate the isosteric heat of adsorption using also the data at 77 K, (fully reversible isotherm, see Fig. S7) and immediately after a 3 point BET measurement at 77 K using N_2 was executed (see Fig. S8), in order to check again the porosity. The later revealed a low BET area of 50 $m^2\ g^{-1}$ suggesting again limited accessible porosity. Taking into account the fact that the material after recording all gas-sorption isotherms, including ammonia, is stable (see pxrd in Fig. S1d), the pore blockage upon gas-sorption of small and inert molecules like H_2, is attributed to the strong confinement of the guest species inside the ultramicropores of **1'**. Presumably, a small amount remains inside that is blocking the pores.

As shown in Fig. 4, the hydrogen saturation uptake is 131.1 $cm^3\ g^{-1}$ (1.2 wt%) at 27 bar and 77 K (110.3 $cm^3\ g^{-1}$ or 1.0 wt% at 1 bar and 77 K) which is higher compared to the reported values for other microporous Mg-formates (1.1 wt% for α-

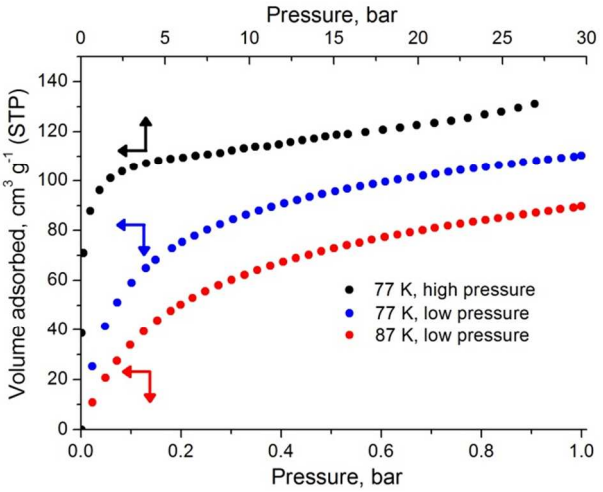

Fig. 4 High and low pressure H_2 adsorption isotherms of **1'** recorded at the indicated temperatures.

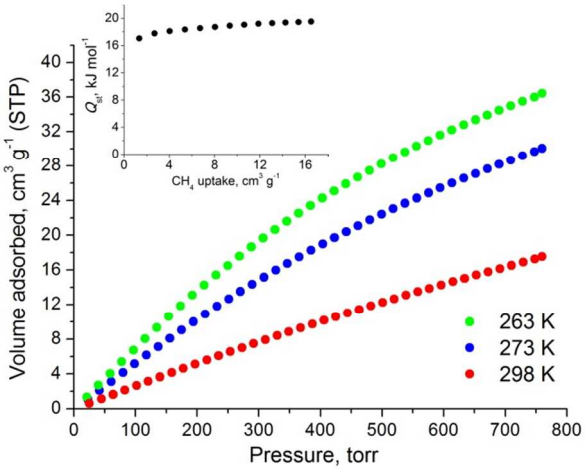

Fig. 6 Low pressure CH_4 adsorption isotherms recorded at the indicated temperatures. Inset shows the calculated isosteric heat of adsorption using the Clausius-Clapeyron equation.

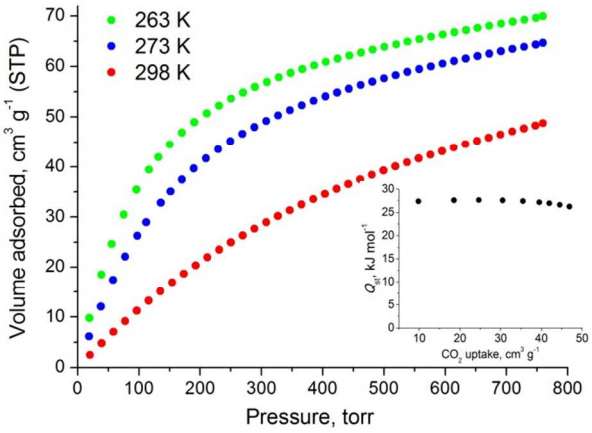

Fig. 5 Low pressure CO_2 adsorption isotherms recorded at the indicated temperatures. Inset shows the calculated isosteric heat of adsorption using the Clausius-Clapeyron equation.

$[Mg_3(O_2CH)_6]$[12] and 1.0 wt% for γ-$[Mg_3(O_2CH)_6]$[10]). The corresponding isosteric heat of adsorption, Q_{st}, is 6.0 kJ mol^{-1} for low coverage and decrease to 5.5 kJ mol^{-1} for higher coverage. These values are in the same range for the previously reported Mg-formates.[8,10,28] The slightly higher Q_{st} value (6.5 kJ mol^{-1}) reported by Hirscher et al.[12] is attributed to the smaller pore size of that Mg-formate causing an increase of the overlapping potential from the opposite walls thus leading to stronger interactions with hydrogen molecules.[29]

The CO_2 isotherms recorded up to 1 bar revealed an uptake of 69.9 cm^3 g^{-1} (3.1 mmol g^{-1}), 64.7 cm^3 g^{-1} (2.9 mmol g^{-1}) and 48.8 cm^3 g^{-1} (2.2 mmol g^{-1}) at 263 K, 273 K and 298 K respectively, see Fig. 5. The measured uptake at 298 K is the highest among all Mg-formates reported up to date[8,28,30] and reflects the combination of the high surface area with the ultramicropore nature of **1'** (increased framework CO_2-interaction, Q_{st}, as we present below). It is also higher compared to some representative and important porous solids for gas separation application such as BPL activated carbon (2.1 mmol g^{-1}) and ZIF-8 (0.8 mmol g^{-1}) under the same experimental conditions.[31] At high pressures, the saturation CO_2 uptake is 3.8 mmol g^{-1} at 273 K/35 bar, 3.1 mmol g^{-1} at 293 K/35 bar and 2.9 mmol g^{-1} at 303 K/32.5 bar, see Fig. S17. The corresponding isosteric heat of adsorption, Q_{st}, calculated from the low pressure isotherms at the three different temperatures using the Clausius-Clapeyron equation, is 27.4 kJ mol^{-1} at low CO_2 coverage, then slightly increases to 27.7 kJ mol^{-1} and finally drops to 26.3 kJ mol^{-1} at higher loadings, see inset in Fig. 5. These are among the highest Q_{st} values that have been reported for MOFs without strong polarizing sites or basic functional groups[32] and comparable with MOFs having unsaturated metal sites. For example NOTT-104, a MOF with open Cu^{2+} sites, has a value of 25 kJ mol^{-1}.[33] The observed increase in Q_{st} as a function of surface coverage is unusual and more pronounced for CH_4 adsorption, as we discuss below.

The CH_4 adsorption isotherms up to 1 bar, shown in Fig. 6, revealed an uptake of 36.4 cm^3 g^{-1} (1.6 mmol g^{-1}), 30.1 cm^3 g^{-1} (1.3 mmol g^{-1}) and 17.5 cm^3 g^{-1} (0.8 mmol g^{-1}) at 263 K, 273 K and 298 K, respectively. The saturation uptake at high pressures is 1.8 mmol g^{-1} at 303 K/ 26.5 bar, 1.96 mmol g^{-1} at 293 K/24 bar and 2.11 mmol g^{-1} at 273 K/27 bar, see Fig. S18. For comparison purposes with literature data, the saturation volumetric uptake at 293 K/24 bar is 58.6 cm^3 cm^{-3}. This is a moderate value due to the relatively low surface area of **1'** as compared to other MOFs targeted for methane storage,[34] such as PCN-14 and HKUST-1.[35] The corresponding isosteric heat of adsorption (shown in inset of Fig. 6) is 17.1 kJ mol^{-1} at low CH_4 coverage and surprisingly, increases with increasing CH_4 uptake reaching 19.5 kJ mol^{-1} (12.3% increase) at high loadings. This is a rare observation in MOFs[36] and other microporous materials[37] indicating that methane-methane interactions becomes progressively more significant within the adsorption layer, due to the small pore size in **1'**.[38,39] The observed Q_{st} values are among the highest in MOFs without unsaturated metal sites[34,35], resulting in a high CH_4/N_2 selectivity at room temperature as we describe below.

The calculated CO_2/CH_4 selectivity at low pressures, using the IAST model at 298 K for a 5/95 molar mixture is 4.65 and remains constant as a function of pressure, see Fig. 7. This is a

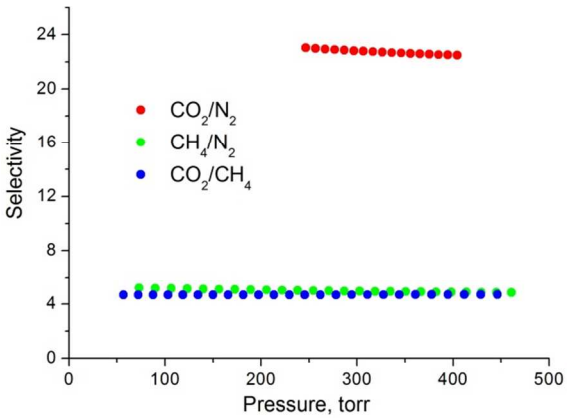

Fig. 7 IAST CO_2/N_2, CH_4/N_2 and CO_2/CH_4 selectivity at 298 K calculated from the corresponding pure adsorption isotherms.

moderate selectivity compared to other MOFs[40] having strong polarizing groups or unsaturated metal sites, however is higher compared to some well-known microporous materials such as BPL activated carbon (2.75) and ZIF-8 (3.8), under similar experimental conditions.[31] The corresponding CO_2/N_2 and CH_4/N_2 selectivity is 23.03 and 5.17, respectively and remains almost constant as a function of pressure. The CO_2/N_2 selectivity is among the highest in MOFs with no open metal sites or amines groups but lower compared to the best performing materials.[32,41,42] However, the CH_4/N_2 selectivity is among the highest ever reported[43] for porous materials, indicating that **1'** is a very promising candidate for the separation of N_2 from CH_4 in natural gas. For comparison, the commercially available Al-BDC MOF (Basolite A100) shows selectivity between 3.3-4.4[44], a copper triazolyl based-MOF 4.0-5.0[44] and HKUST-1 2.9-3.1.[45] Interestingly, the best performing material so far is a Ni-formate with a reported selectivity at 298 K of 6.1.[43] It is important to note here that CH_4/N_2 separation is one of the most challenging processes due to the very similar properties of these two gases.[46,47] The observed gas selectivities are attributed to the different electronic properties[48] (i.e. quadrupole moment and polarizability) of the gases and the fact that **1'** has ultramicropores (increased overlapping potential) with polar walls. Accordingly, CH_4 adsorbs preferentially over N_2 due to its higher polarizability (26.0 x 10^{-25} cm^3 for CH_4 versus 17.6 x 10^{-25} cm^3 for N_2) while CO_2 adsorbs preferentially over N_2 and CH_4 due to its large quadrupole moment (13.4 x 10^{-40} C m^2 for CO_2, 4.7 x 10^{-40} C m^2 for N_2, CH_4 is non-polar).[49]

Finally, we evaluated the NH_3 sorption properties of **1'** by recording isotherms at 273 K and 298 K up to 1 bar, were a reversible uptake of 141.7 cm^3 g^{-1} (6.33 mmol g^{-1}) and 120.2 cm^3 g^{-1} (5.37 mmol g^{-1}), respectively is observed, see Fig. S20. The uptake at 298 K is higher compared to some representative solids having a high density of unsaturated metal sites, such as Zn-MOF-74 and Ni-MOF-74[50] but lower than the record values reported for MOFs and COFs.[51] However, it is very important to note that the material is stable after 3 cycles (two performed at 298 K and one at 273 K) as confirmed by PXRD, see Fig. S1d.

CONCLUSIONS

A simple synthesis and the successful pore activation of *α*-$[Mg_3(O_2CH)_6](DMF)$ (magnesium formate) with an expanded unit cell is reported. Accordingly, we found that a thermal treatment at 240 ^oC under vacuum is important in order to properly activate the material and access its full surface area. The measured surface of 496 m^2 g^{-1} is the highest among all the reported magnesium formates. The activated material exhibits ultramicroporosity with 4.8 Å pore width and is found to be stable even after exposure to NH_3. Extensive gas-sorption study was executed, revealing a high CH_4/N_2 selectivity at 298 K (5.2), rendering this material a potential candidate for this important gas separation application. Ammonia uptake is also high reaching 5.37 mmol g^{-1} at 298 K and 1 bar. The corresponding CO_2 uptake was found to be 2.2 mmol g^{-1} with moderate CO_2/CH_4 (4.65) but high CO_2/N_2 (23.03) selectivity. We are currently exploring the possibility to construct membranes from this MOF and study the corresponding gas-separation properties.

Acknowledgements

This research has been co-financed by the European Union (European Social Fund–ESF) and Greek national funds through the Operational Program "Education and Lifelong Learning" of the National Strategic Reference Framework (NSRF)-Research Funding Program: Aristeia II 4862.

Notes and references

[a] *Department of Chemistry, University of Crete, Voutes 71003 Heraklion, Greece. Email: ptrikal@chemistry.uoc.gr; Tel.: +30 2810 545052.*
[b] *National Center for Scientific Research Demokritos, Terma Patriarchou Gregoriou & Neapoleos, Athens 15310, Greece.*
[c] *University of Cyprus, Department of Chemistry, CY-1678 Nicosia, Cyprus.*

† Electronic Supplementary Information (ESI) available: [pxrd, ^1H NMR, TGA and additional gas-sorption data]. See DOI: 10.1039/b000000x/

1 A very recent themed issue in Chemical Society Reviews on Metal Organic Frameworks (MOFs), guest edited by Susumu Kitagawa and Hong-Cai "Joe" Zhou, covers very well the current state-of-the-art in the field.
2 C. Wang, D. Liu, W. Lin, *J. Am. Chem. Soc*., 2013, 135, 13222.
3 T. M. McDonald, W. R. Lee, J. A. Mason, B. M. Wiers, C. Hong, J.R. Long, *J. Am. Chem. Soc*., 2012, 134, 7056.
4 H. Reinsch, M. Krüger, J. Wack, J. Senker, F. Salles, G. Maurin, N. Stock, *Micropor. Mesopor. Mater.*, 2012, 157, 50.
5 B. Chen, N. W. Ockwig, A. R. Millward, D. S. Contreras, O. M. Yaghi, *Angew. Chem., Int. Ed.*, 2005, 44, 4745.
6 L. Schlapbach, A. Zuttel, Nature, 2001, 414, 353.
7 S. R. Caskey A. G. Wong-Foy, A.J. Matzger, *J. Am. Chem. Soc.*, 2008, 130, 10870.
8 J. A. Rood, B. C. Noll, K. W. Henderson, *Inorg. Chem.*, 2006, 45, 5521.
9 M. Viertelhaus, C. E. Anson, A. K. Powell, *Z. Anorg. Allg. Chem.*, 2005, 631, 2365.
10 A. Mallick, S. Saha, P. Pachfule, S. Roy, R. Banerjee, *Inorg. Chem.*, 2011, 50, 1392.

11 Basosiv™ M050 produced by BASF, available from Aldrich.
12 B. Schmitz, I. Krkljus, E. Leung, H. Hoffken, U. Muller, M. Hirscher, *ChemSusChem*, 2010, 3, 758.
13 H. Kim, D. G. Samsonenko, M. Yoon, J. W. Yoon,Y. K. Hwang, J.-S. Chang, K. Kim, *Chem. Commun*. 2008, 4697.
14 The lower calculated surface area is acceptable within the error of the applied methodology (a probe molecule rolling along the surface of the material, see reference #25).
15 Sheldrick, G. M. *Act. Cryst*. 2008, A64, 112−122.
16 Oxford Diffraction. CrysAlis CCD and CrysAlis RED; Oxford Diffraction Ltd: Abingdon, Oxford, England, 2008.
17 Burla, M. C.; Caliandro, R.; Camalli, M.; Carrozzini, B.; Cascarano, G. L.; De Caro, L.; Giacovazzo, C.; Polidori, G.; Spagna, R. *J. Appl. Crystallogr*. 2005, 38, 381−388.
18 Farrugia, L. J. *J. Appl. Crystallogr*. 1999, 32, 837−838.
19 http://www.ccdc.cam.ac.uk/
20 S. Yang, X. Lin, A. J. Blake, K. M. Thomas, P. Hubberstey, N. R. Champness, M. Schroder, *Chem. Commun*., 2008, 6108.
21 A.L.Spek (2005) PLATON, A Multipurpose Crystallographic Tool, Utrecht University, Utrecht, The Netherlands.
22 Monoclinic system, space group *P*21/n, a = 11.3630(5) Å, b = 9.8950(5) Å, c = 14.6054(8) Å, β = 91.441(4)º, V = 1641.67(14) Å3, Z = 4, ρ_{calc} = 1.388 g cm^{-3}, T=250(2) K, $2\theta_{max}$ = 66.94º. Refinement of 217 parameters on 2908 independent reflections out of 5659 measured reflections (R_{int} = 0.0343) led to R_1= 0.0443 (I > 2σ(I)), wR_2 = 0.1043 (all data) and S = 1.002 with the largest difference peak and hole 0.324 and -0.385 e.Å^{-3}. The very low remaining electron density is in agreement with the fact that **1'** is solvent-free.
23 A. P. Nelson, O. K. Farha, K. L. Mulfort, J. T. Hupp, *J. Am. Chem. Soc*. 2009, 131, 458.
24 B. Liu, A. G. Wong-Foy, A. J. Matzger, *Chem. Commun*., 2013, 49, 1419.
25 T. Düren, F. Millange, G. Ferey, K.S. Walton, R.Q. Snurr, *J. Phys. Chem. C*, 2007, 111, 15360.
26 Characterization of Porous Solids and Powders: Surface Area, Porosity and Density; S. Lowell, J. Shields, M.A. Thomas & M. Thommes, Springer, (2004).
27 We note that the unit cell volume of the BASF sample (1617 Å^3) corresponds to the as-made solid, as reported in reference 12.
28 G. D. Samsonenko, H. Kim, Y. Sun, H. Kim, H. Lee, K. Kim, *Chem. Asian J.*, 2007, 2, 484.
29 M. Dinca, A. Dailly, Y. Liu, C.M. Brown, D. A. Neumann, J. R. Long, J. *Am. Chem. Soc*., 2006, 128, 16876.
30 A. Rossin, A. Ienco, F. Costantino, T. Montini, B. Credico, M. Caporali, L. Gonsalvi, P. Fornasiero, M. Peruzzini, *Cryst. Growth Des.,* 2008, 8, 3302.
31 J. McEwen, J.-D. Hayman and A. O. Yazaydin, *Chem. Phys.* 2013, 412, 72.
32 K. Sumida, D. L. Rogow, J. A. Mason, T. M. McDonald, E. D. Bloch, Z. R. Herm, T.-H. Bae, J. R. Long, *Chem. Rev*. 2012, 112, 724.
33 C. Tan, S. Yang, N. R. Champness, X. Lin, A. J. Blake, W. Lewis, M. Schroder, *Chem. Commun*., 2011, 47, 4487.
34 Y. He, W. Zhou, G. Qian, B. Chen, Chem. Soc. Rev., 2014,43, 5657.
35 Y. Peng, V. Krungleviciute, I. Eryazici, T. J. Hupp, K. O. Farha, T. Yildirim, *J. Am. Chem. Soc*., 2013, 135, 11887.
36 K. Sillar, J. Sauer, *J. Am. Chem. Soc*., 2012, 134, 18354.
37 N. P. Stadie, M. Murialdo, C. C. Ahn, B. Fultz, *J. Am. Chem. Soc*. 2013, 135, 990.
38 J. A. Mason, M. Veenstra, J. R. Long, *Chem. Sci.*, 2014, 5, 32.
39 J. Moellmer, E.B. Celer, R. Luebke, A.J. Cairns, R. Staudt, M. Eddaoudi, M. Thommes, Micropor. Mesopor. Mater. 2010, 129 345.
40 I. Spanopoulos, P. Xydias, C. D. Malliakas, P. N. Trikalitis, *Inorg. Chem., 2013*, 52, 855.
41 P. Nugent, Y. Belmabkhout, S. D. Burd, A. J. Cairns, R. Luebke, K. Forrest, T. Pham, S. Q. Ma, B. Space, L. Wojtas, M. Eddaoudi, M. J. Zaworotko, *Nature* 2013, 495, 80.
42 D. X. Xue, A. J. Cairns, Y. Belmabkhout, L. Wojtas, Y. Liu, M. H. Alkordi, M. Eddaoudi, *J. Am. Chem. Soc*. 2013, 135, 7660.
43 X. Ren, T. Sun, J. Hu, S. Wang, *Micropor. Mesopor. Mater*. 2014, 186, 137.
44 J. Moellmer, M. Lange, A. Moeller, C. Patzschke, K. Stein, D. Laessig, J. Lincke, R. Glaeser, H. Krautscheid, R. Staudt, *J. Mater. Chem*. 2012, 22, 10274.
45 B. Liu, B. Smit, *Langmuir* 2009, 25, 5918.
46 M. Tagliabue, D. Farrusseng, S. Valencia, S. Aguado, U. Ravonb, C. Rizzo, A. Corma, C. Mirodatos, *Chem. Eng. J*. 2009, 155, 553.
47 D. M. Ruthven, *Ind. Eng. Chem. Res.* 2000, 39, 2127.
48 D. M. D'Alessandro, B. Smit, and J. R. Long, *Angew. Chem. Int. Ed.* 2010, 49, 6058 – 6082.
49 P. Chowdhury, C. Bikkina, S. Gumma, *J. Phys. Chem. C* 2009, 113, 6616.
50 T. G. Glover, G. W. Peterson, B. J. Schindler, D. Britt, O. M. Yaghi, *Chem. Eng. Sci.*, 2011, 66, 163.
51 C. J. Doonan, D. J. Tranchemontagne, T. G. Glover, J. R. Hunt, O. M. Yaghi, *Nature Chem*., 2010, 2, 235.

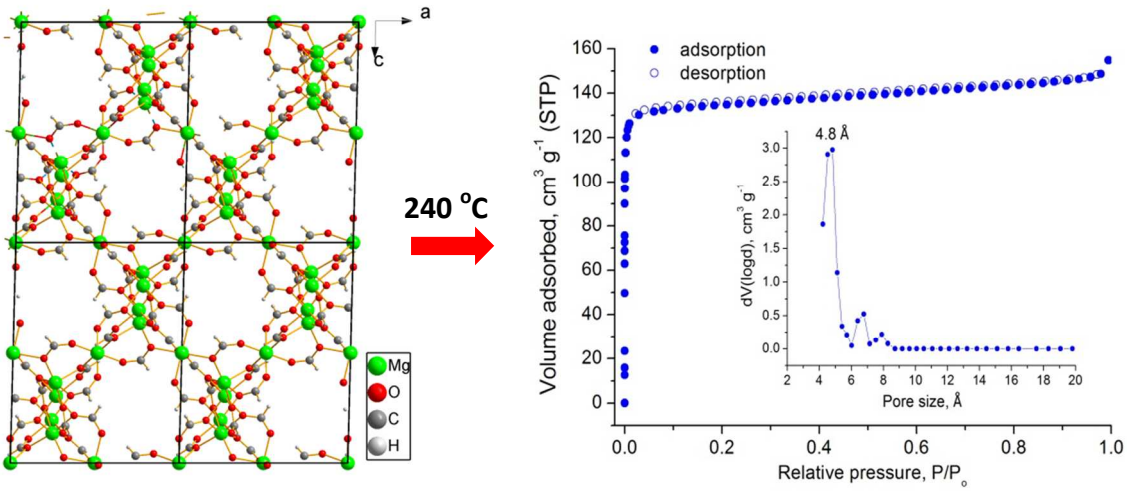

The gas-sorption properties of a high surface area α-magnesium formate with an expanded unit cell, are reported. The material is stable in NH_3, and shows very high CH_4/N_2 (5.2) selectivity.